frontiers | Frontiers in Chemistry

TYPE Mini Review
PUBLISHED 25 October 2022
DOI 10.3389/fchem.2022.1048504

OPEN ACCESS

EDITED BY
Kezhen Qi,
Shenyang Normal University, China

REVIEWED BY
Xin Ying Kong,
Nanyang Technological University, Singapore
Feng Guo,
Jiangsu University of Science and Technology, China

*CORRESPONDENCE
Hang Cong,
ecnuc@163.com
Yun-Qian Zhang,
sci.yqzhang@gzu.edu.cn

SPECIALTY SECTION
This article was submitted to Photocatalysis and Photochemistry, a section of the journal Frontiers in Chemistry

RECEIVED 19 September 2022
ACCEPTED 14 October 2022
PUBLISHED 25 October 2022

CITATION
Gao R-H, Ge Q, Jiang N, Cong H, Liu M and Zhang Y-Q (2022), Graphitic carbon nitride (g-C_3N_4)-based photocatalytic materials for hydrogen evolution. *Front. Chem.* 10:1048504. doi: 10.3389/fchem.2022.1048504

Graphitic carbon nitride (g-C_3N_4)-based photocatalytic materials for hydrogen evolution

Rui-Han Gao[1,2], Qingmei Ge[1], Nan Jiang[1], Hang Cong[1]*, Mao Liu[1] and Yun-Qian Zhang[1,2]*

[1]Enterprise Technology Center of Guizhou Province, Guizhou University, Guiyang, China, [2]Key Laboratory of Macrocyclic and Supramolecular Chemistry of Guizhou Province, Guizhou University, Guiyang, China

The semiconductors, such as TiO_2, CdS, ZnO, $BiVO_4$, graphene, produce good applications in photocatalytic water splitting for hydrogen production, and great progress have been made in the synthesis and modification of the materials. As a two-dimensional layered structure material, graphitic carbon nitride (g-C_3N_4), with the unique properties of high thermostability and chemical inertness, excellent semiconductive ability, affords good potential in photocatalytic hydrogen evolution. However, the related low efficiency of g-C_3N_4 with fast recombination rate of photogenerated charge carriers, limited visible-light absorption, and low surface area of prepared bulk g-C_3N_4, has called out the challenge issues to synthesize and modify novel g-C_3N_4-block photocatalyst. In this review, we have summarized several strategies to improve the photocatalytic performance of pristine g-C_3N_4 such as pH, morphology control, doping with metal or non-metal elements, metal deposition, constructing a heterojunction or homojunction, dye-sensitization, and so forth. The performances for photocatalytic hydrogen evolution and possible development of g-C_3N_4 materials are shared with the researchers interested in the relevant fields hereinto.

KEYWORDS

g-C3N4, photocatalysis, hydrogen evolution, energy materials, semiconductor

1 Introduction

With the development and progress of human society, environmental pollution and energy shortage have become two major problems that plague human beings. Hydrogen is considered as one of the best candidates for storing solar energy meeting the growing clean energy demand (Chen et al., 2016; Shen et al., 2016; Wang et al., 2016; Wu et al., 2017; Wang et al., 2018; Liu et al., 2019). Since Fujishima and Honda discovered the hydrogen evolution reaction activates by TiO_2 under irradiation in 1972, photocatalytic water splitting is one of the promising means for hydrogen production (Fujishima and Honda., 1972). Without relying on fossil reserves, the photocatalytic hydrogen evolution from water with highly efficient utilization of solar irradiation is a desirable exploration for the solution of the energy issues (Maeda et al., 2006; Qi et al., 2022). Although great

process in photocatalysts of water splitting have been made for H_2 evolution under visible light, there are still challenging and concerns with semiconductors to promise hydrogen energy development methods (Zhong et al., 2015; Wang et al., 2016; Zhang et al., 2018; Qi et al., 2020).

Graphitic carbon nitride (g-C_3N_4) is considered as an ideal 2D material with the conjugated skeleton for photocatalytic water splitting with the activity of photoelectronic chemistry and high stability in the photochemical reaction (Ong et al., 2016). Compounds in rich carbon and nitrogen elements such as melamine, urea, cyanamide, dicyandiamide, cyanuric acid, etc. are usually subjected as the precursors. Graphitic carbon nitride materials were synthesized by methods including electrochemical deposition, thermal shrinkage polymerization, solid phase synthesis, gas phase synthesis, solvothermal synthesis and electrochemical deposition (Thomas et al., 2008). Under light irradiation, electron-hole pairs were generated on the surface of g-C_3N_4 photocatalyst to provide the reaction sites. The water molecules adsorbed on the surface of g-C_3N_4 undergo the photocatalytic reduction for H_2 evolution and oxidation for O_2 release, respectively, with the efficacious charge carriers by the reactions (1–3):

Oxidation:

$$H_2O + 2h^+ \rightarrow 2H^+ + 1/2O_2 \quad (1)$$

Reduction:

$$2H^+ + 2e \rightarrow H_2 \quad (2)$$

Overall reaction:

$$H_2O \rightarrow H_2 + 1/2O_2 \quad (3)$$

The first case of g-C_3N_4 as a polymeric photocatalyst for water splitting to produce H_2 under visible-light irradiation was reported by Wang et al. (Wang et al., 2009) Figure 1 schematically described the photogeneration of H_2 and O_2 in water splitting reaction with the pristine g-C_3N_4. The obtained bulk form of g-C_3N_4 exhibited some drawbacks including limited visible light utilization efficiency, fast recombination rate of photogenerated electron-hole pairs, and low specific surface areas (<10 m^2g^{-1}), which still limited the photocatalytic performance of on its practical applications (Reza et al., 2015; Fu et al., 2018), and modification of g-C_3N_4 has been recognized to be the effective way to improve the photocatalytic performance of pristine g-C_3N_4.

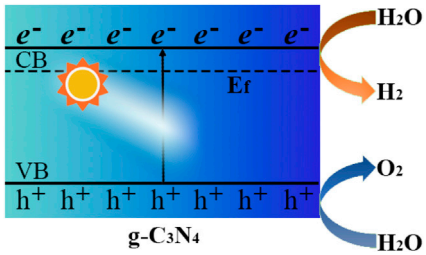

FIGURE 1
Schematic of generation of H_2 and O_2 from water with the catalysis of pristine g-C_3N_4 under light irradiation.

2 Modification of graphitic carbon nitride materials

Recently, the application of g-C_3N_4 with improved photocatalytic performance by developed several strategies, involving adjusting pH value, morphology control, doping by heteroatoms or metals, participation of co-catalyst, dye-sensitization, and construction of heterojunction. The hydrogen evolution performance of the modified g-C_3N_4-based materials are summarized in Table 1 to provide the development of the co-catalysts in the photolysis system.

2.1 pH

The pH value of solution was an important factor affecting the activity of g-C_3N_4, that is, Zeta potential values suggested the surface charge of g-C_3N_4 could be changes at different pH value for the diversity of functional groups on the surface (Wang et al., 2016). Wu et al. demonstrated that the alkaline environment was beneficial to the photocatalytic hydrogen evolution efficiency of g-C_3N_4 material as shown in Figure 2A (Wu et al., 2014). The experimental results show that pH and methanol have certain effects on the photocurrent amplification on g-C_3N_4 films. In the presence of methanol, the photoelectronic efficiency was improved to provide an increased photocurrent from 0.6 to 1.2 μA cm^{-2}, which was further enhanced to offer a 4.2 μA cm^{-2} current upon adding base to bring the pH to 12.8. The results implied the transfer of photogenerated holes into solution was enhanced by the addition of methanol and alkali, which could root in the additive-induced decrease of the energy gap of the flat band and band-edge of g-C_3N_4 as description in Figure 2B, that is, methanol oxidation occurred in alkaline solution, but restrained in acidic condition with the amine-terminated g-C_3N_4 surface.

2.2 Morphology control

The activity of g-C_3N_4 for H_2 production *via* water splitting under visible-light irradiation could be determined by morphology of the material surface (Niu et al., 2012; Zhang et al., 2012; Han et al., 2015). The targets of controllable morphologies in preparation of well-defined g-C_3N_4 nanostructures to get larger specific surface area and more

TABLE 1 Hydrogen evolution performance of the modified g-C_3N_4-based materials.

Methods	Co-catalysts	Hydrogen evolution rate (μmol $h^{-1}g^{-1}$)	Ref.
0D	Quantum dots	2,199.2	Wang et al. (2014)
1D	Nanotubes	11,850	Mo et al. (2018)
2D	Nanosheets	3,140	Zhao et al. (2018)
3D	Nanovesicles	10,300	Sun et al. (2022a)
Non-metal doping	P dopant	1,596	Ran et al. (2015)
Metal doping	Co dopant	560	Chen et al. (2017)
Metal deposition	Pt co-catalyst	947.64	Zhu et al. (2019)
Dye sensitization	Protoporphyrin	1,153.8	Liu et al. (2020)
Heterogeneous	CeO_2	1,240.9	Zhao et al. (2021)
Homojunction	High-crystalline g-C_3N_4	5,534	Sun et al. (2022b)

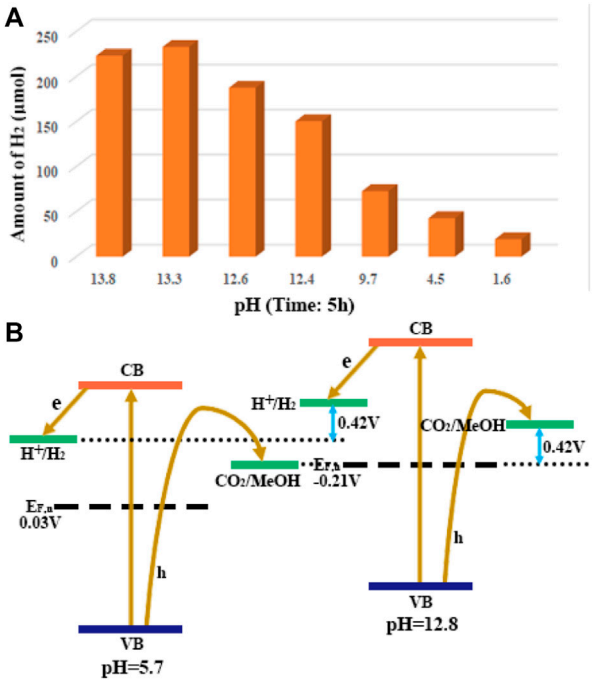

FIGURE 2
(A) the relationship of pH values to the efficiencies of H_2 evolution with g-C_3N_4 photolysis; **(B)** energy diagrams of g-C_3N_4 in solution at pH 5.7 and 12.8.

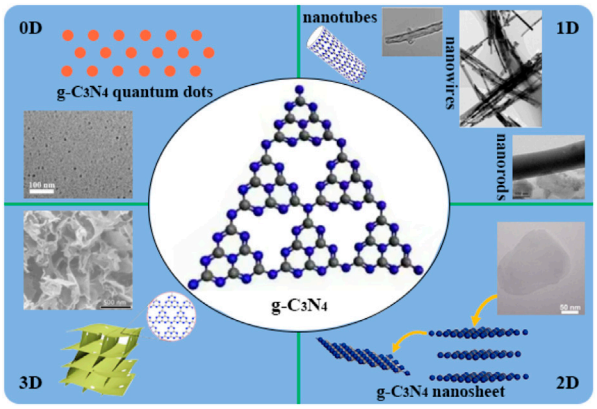

FIGURE 3
Schematic illustration of 0D, 1D, 2D and 3D g-C_3N_4.

abundant reactive sites, reduced the recombination rate of photogenerated charge carriers. There were different nanostructures of g-C_3N_4 have been described in pioneering reports involving zero-dimensional (Wang et al., 2014) (0D), one-dimensional (Bai et al., 2013; Zhang et al., 2013; Wang et al., 2015; Mo et al., 2018; Bashir et al., 2019; Zhang et al., 2020) (1D), two-dimensional (Li et al., 2015; Zhao et al., 2018; Qi et al., 2019; Shi et al., 2022) (2D), three-dimensional (Li et al., 2016; Di et al., 2018; Chen et al., 2019) (3D) as shown in Figure 3, which built an ideal platform for collectively advanced photoredox processes for the enormous advantages in terms of physical and chemical characterization in following details.

The photocatalytic performance of 0D nanostructured materials are dependence on the natures including quantum size effect, small size effect, surface effect, macroscopic quantum effect and so on. Prof. Yu and co-workers prepared graphitic carbon nitride quantum dot structures directly from g-C_3N_4 with a thermochemical etching process, which produced unique upconversion properties and higher hydrogen production efficiency than original g-C_3N_4 in 2.87 times (Wang et al., 2014).

There was more explosion of active sites on the surface of 1D g-C_3N_4, which was reported as nanotubes (Mo et al., 2018; Guo et al., 2021), nanowires (Zhang et al., 2013; Wang et al.,

2015), nanorods (Bai et al., 2013; Bashir et al., 2019) and so on, and efficient transfer of photogenerated electrons could be realized along one-dimensional paths with enhancement of visible light absorption and fast short-distance electron transport. Mo et al. developed g-C_3N_4 nanotubes with large number of nitrogen defects by a green-, acid- and base-free synthesis method, and the hydrogen production of 118.5 μmol h^{-1} was far superior to pristine g-C_3N_4 (Mo et al., 2018).

Compared with 1D structures, 2D photocatalysts have greater potential because of their larger specific surface area and thinner thickness, exposing more active sites and shortening the transport path of photogenerated carriers. Prof. Zhu's group successfully fabricated g-C_3N_4 nanosheets with a single atomic layer structure of only 0.4 nm thickness, with a simple chemical exfoliation method. The single-atom-layer nanosheets offered better separation and transfer rates of photogenerated carriers, and exhibited higher performance than bulk g-C_3N_4 in photocatalytic splitting of water for hydrogen production and photocurrent generation. Chen's group proposed that the precursors assembled into nanorods at low power level, while grew into nanoplates at high power level, which implied that the morphology of g-C_3N_4 was dependance upon on a kinetically driven process (Li et al., 2015). Zhao et al. treated supramolecular precursors under the action of glycerol and ethanol to obtain porous few-layer g-C_3N_4 (Zhao et al., 2018). The hydrogen evolution rate of thin-layer g-C_3N_4 was evaluated to be 159.8 μmol h^{-1}, as the results of its large specific surface area, more active sites, and the abundant nitrogen vacancies in the framework, to accelerate the transfer of photogenerated electrons.

Compared with 2D g-C_3N_4 nanosheets, the porous 3D g-C_3N_4 material can provide a larger specific surface area. It also maximizes the use of incident photons through multiple reflections within the interconnected open frame (Di et al., 2018). In addition, the porous 3D g-C_3N_4 material acted as a support to prevent the agglomeration of ultrathin nanosheets and provided a pathway for electron transfer, thereby greatly enhancing the photocatalytic activity (Li et al., 2016). Zhang et al. utilized a simple bottom-up supramolecular self-assembly route to assemble a porous 3D g-C_3N_4 with high crystallinity and applied it to photocatalytic water splitting (Chen et al., 2019). In 2022, Guo et al. reported a facile template-free self-assembly method to synthesize three-dimensional porous g-C_3N_4 nanovesicles for achieving efficient and durable photocatalytic generation of H_2, and the large-size vesicles exhibited the high H_2 production rate of 10.3 mmol h^{-1} g^{-1} (Sun et al., 2022). And 3D onion-ring-like g-C_3N_4 was made from silica microsphere as a hard-template, which afforded excellent properties such as large specific surface area, strong optical absorption, high dispersion, for the efficient water splitting with 5-fold higher than that of pristine g-C_3N_4 (Cui et al., 2018; Shi et al., 2022).

2.3 Doping

Graphitic carbon nitride, as a conjugated polymeric material with a band gap of about 2.7 eV, has a relatively narrow response to visible-light. Numerous research results suggested that the optical properties and some other physical properties of g-C_3N_4 could be well regulated by doping foreign elements (Chen et al., 2017; Zeng et al., 2018; Fang et al., 2019; Sun H.,R. et al., 2022a). Therefore, the photocatalytic activity of pure g-C_3N_4 could be improved by hybridization with a small amounts of non-metals or metals into the framework.

2.3.1 Non-Metal doping

Hybridization of non-metallic dopants such as B, S, O, P and I to realize the ingenious design of the electronic structure, was considered as an important method for the improvement of g-C_3N_4 performance (Qi et al., 2021). Non-metal doping refers to doping of some non-metal elements into the structural framework, which not only modified the electronic and textural properties of g-C_3N_4 photocatalyst, but also improved the separation efficiency of photogenerated charge carriers and finally boosted the photocatalytic activity. Fang and coworkers (Fang et al., 2019) reported P-doped g-C_3N_4 for photocatalytic water splitting, and 4-(diphenylphosphino)benzoic acid (4-DPPBA) was employed as the precursor of phosphorous. The combination of P-doping and thermal exfoliation was applied for the preparation of porous g-C_3N_4 with P hybridization, which afford excellent photocatalysis for hydrogen evolution high to 1,596 μmol h^{-1} g^{-1} under irradiation of visible light (Ran et al., 2015). As demonstrated by DFT and experimental studies, the empty intermediate bandgap state enhanced the photo sensitivity with P hybridization, and the mass transfer process and light trapping were improved on the macroporous structure. The intrinsic energy gap of g-C_3N_4 was decrease from 2.98 to 2.66 eV in the attendance of P dopant. On the other hand, Lin and co-workers discovered the B,F-doped g-C_3N_4 porous nanosheets were achieved by the self-polymerization of urea in the presence of ionic liquid [Bmim][BF_4], which yielded photocatalytic hydrogen in 3.9 times higher than pristine g-C_3N_4 (Lin and Wang., 2014) (Zhang et al., 2014). successfully obtained iodine-doped carbon nitride (CN-I) with calcining dicyandiamide to significantly improve the hydrogen production performance (Zhang et al., 2014). The photocatalytic activity of iodine-doped g-C_3N_4 was occurred at the wavelength of 600 nm, while pristine g-C_3N_4 provided inactive catalysis at 500 nm. Guo et al. (Guo et al., 2016) prepared a phosphorus-doped hexagonal hollow tubular structure g-C_3N_4 by hydrothermal method and the special structure greatly increased the specific surface area of the catalyst, thereby increasing the number of active sites for hydrogen production. Carbon doping is also an important part of non-metal dopants. In 2021, Liu et al. reported the synthesis of C-doped g-C_3N_4 by one-step copolymerization using melamine and chitosan as the

raw materials (Liu et al., 2021). The N atom in g-C_3N_4 matrix was replaced by C to form the delocalized big Π bonds. The prepared C-doped g-C_3N_4 exhibited an excellent photocatalytic H_2 evolution activity of 1,224 mmol h^{-1} g^{-1}, which was 4.5 times than the free g-C_3N_4.

2.3.2 Metal doping

In addition to the doping of non-metallic elements, the g-C_3N_4 framework was also doped with metallic elements to modify the electronic energy band structure, thereby improving the visible-light absorption, and enhancing the migration and separation of photogenerated carriers in the g-C_3N_4 photocatalyst (Chen et al., 2016). reported the Co-doped g-C_3N_4 synthesized by one-step thermal polymerization of cobalt phthalocyanine (CoPc) and melamine as the precursors (Chen et al., 2017). Yue et al. used a simple chemical method to dope metallic Zn into g-C_3N_4 (Yue et al., 2011). When the content of Zn was 10%, the visible-light-generated hydrogen production activity was 10 times higher than the pure g-C_3N_4. The proposed mechanism implied that doping of Zn increased the light absorption, improved the separation efficiency of electron-hole pairs, and enabled more electrons for water splitting. However, it is still a challenge to obtain nanoparticles with uniform size, regular shape, and high stability with common precursors such as polymers, carbon supports, ionic liquids, surfactants and microemulsions. In the recent report of our group, the coordination complex of cucurbit [6]uril and Co^{2+} was developed as the precursor, to produce cobalt nanoparticles with themolysis, for photocatalytic electrolysis of water by deposition on the surface of the g-C_3N_4 film. (Dai et al., 2022). The formed semiconductor-metal interface provided more reaction sites and electron transport channels for effective charge carriers to capture photons and excite electrons, thereby, promoting the photoelectrocatalytic reaction process. The discovery provided a new strategy for exploring macrocyclic/g-C_3N_4 materials with excellent photocatalytic activities.

2.4 Metal deposition (co-catalyst)

Various studies suggested that metal deposition on pure g-C_3N_4 was also one of the promising methods to enhance the photocatalytic activity. In theory, when metal nanoparticles are in contact with g-C_3N_4, a Schottky junction is formed at the interface of metal and g-C_3N_4 semiconductor due to the different work function, which changes the electron distribution on the semiconductor surface (Naseri et al., 2017; Caux et al., 2019; Qi et al., 2020; Zhao et al., 2021). The main function of metal is to accept the photogenerated electrons from the CB of g-C_3N_4 during the photocatalytic H_2 production process. Various metals such as Pt (Ou et al., 2017; Zhu et al., 2019), Au (Samanta et al., 2014; Caux et al., 2019),

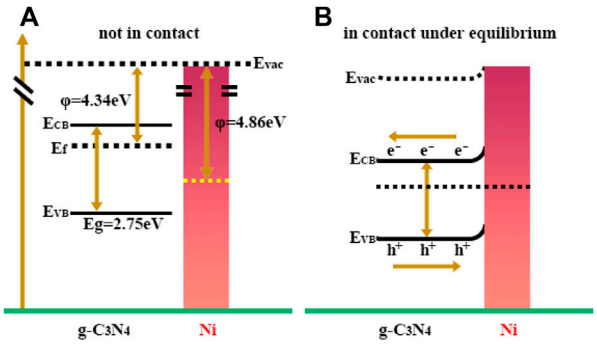

FIGURE 4
Schematic graph shows **(A)** the energy level diagram of g-C_3N_4 and Ni; **(B)** the interfacial electron transfer between g-C_3N_4 and Ni under irradiation.

Pd (Xiao et al., 2019), Ag (Nagajyothi et al., 2017; Deeksha et al., 2021) and Ni (Indra et al., 2016; Kong et al., 2016) were employed as co-catalyst for the efficient sensitization for photocatalysis with the surface plasmon resonance (SPR) effect, which improved the light absorption capacity of the catalyst. With an *in situ* photoreduction, Pt/g-C_3N_4 was subjected to be a visible light photocatalyst by Wang's group, and the results indicated that the photocatalytic hydrogen evolution capability was gradually enhanced as the size decrease of the Pt co-catalyst (Zhu et al., 2019). The participation of Pt provided more active sites on the surface for reduction, which was favorable for accepting electrons from CB of g-C_3N_4, due to the formation of Schottky junctions at the interface of Pt and g-C_3N_4. The PL spectra and UV-vis/DRS spectra of g-C_3N_4 and Pt_x-CN with different Pt content, demonstrated that Pt loading greatly improved charge separation and transfer in g-C_3N_4 photocatalysts, thereby reduced charge recombination, and enhanced photocatalytic activity, as well as provided the maximum utilization efficiency photocatalytic performance for H_2 production. The $Pt_{0.1}$-CN (with 0.1wt% Pt loading amount) sample displayed the highest photocatalytic activity with H_2 evolution of 473.82 μmol mg^{-1} under visible-light irradiation.

Furthermore, Bi et al. reported a Ni cocatalyst for the enhancement of photocatalytic performance of g-C_3N_4 (Bi et al., 2015). A higher separation efficiency of photogenerated charge carriers was obtained as a result of a deeper band bending of g-C_3N_4 contacting with Ni, which contributed to enhanced photocatalytic H_2 production performance. In addition, the heterojunction formed between the Ni nanoparticles and g-C_3N_4 acted as an electron collector, and impeded the recombination rate of photogenerated electron and holes as illumination in Figure 4. Ni/g-C_3N_4 catalyst exhibited high photocatalytic H_2 evolution rate (8.314 μmol h^{-1}) compared

with pristine g-C_3N_4, in which rapid recombination between conduction band (CB) and valence band (VB) holes and the quick reversible reaction occurred.

2.5 Dye sensitization

To overcome the g-C_3N_4 absorption edge of a band gap of 2.7 eV, organic dyes were employed as a driver to improve the visible-light photoactivity (Bard and Fax., 1995; Kudo and Miseki., 2009; Kim et al., 2015), which were considered to dramatically extend the visible-light region of the band-gap of semiconductor (Zhuang et al., 2019). However, the researches about H_2 production based on dye-sensitized carbon nitride were still insufficient, only few organic dyes such as metal-porphyrins (Yu et al., 2014; Chen et al., 2015; Zhang et al., 2015; Zhuang et al., 2019; Liu et al., 2020), poly (3-hexylthiophene) (Zhang et al., 2015), eosin Y (EY) (Min and Liu., 2012; Wang et al., 2018; Qi et al., 2019; Xu et al., 2019; Nagaraja et al., 2020; Zhao et al., 2021) and erythrosin B (ErB) (Wang et al., 2013; Zhang et al., 2017; Zhang et al., 2017) have been successfully applied to enhance the photocatalytic activity with improvement of the utilization efficiency of visible-light. In the process of H_2 generation, the organic dyes were damaged in oxidation reactions, and its stabilization could be realized with a porous support, which accelerates the transfer of electrons from the excited dye molecule to the active site in definition of a cocatalyst, in general use of noble metals (especially Pt). The hybridization of Ag with g-C_3N_4 was applied for hydrogen evolution, and the photocatalysis was improved with the dye-sensitization under visible-light irradiation (Schwinghanmmer et al., 2013). Min et al. reported that g-C_3N_4 with modification of Eosin Y performed the light-drove H_2 generation at about 600 nm, while the reaction occurred at less than 460 nm on the pristine g-C_3N_4 surface (Min and Liu., 2012).

2.6 Heterogeneous structure

The photocatalytic efficiency and application of pristine g-C_3N_4 were limited for high recombination rate of photogenerated charge carriers and narrow range of visible light response in a solar spectrum. Recently, g-C_3N_4-based heterojunctions were developed by enhancement of carrier separation efficiency and demonstrated excellent photocatalytic performance. Semiconductors were induced to form heterojunctions with g-C_3N_4 including carbon materials (graphene (Xiang et al., 2011), carbon nanotubes (Ge and Han., 2012), fullerenes (Chai et al., 2014)), metal oxides (TiO_2(Chen and Liu, 2016), SnO_2(Zada et al., 2019), ZnO(Sun et al., 2012), $NiFe_2O_4$(Liu et al., 2022), Fe_2O_3(Theerthagiri et al., 2014)), metal sulfides (CdS(Chen et al., 2016), ZnS(Shi et al., 2014), MoS_2(Li et al., 2014)), bismuth-based compounds ($BiPO_4$(Zou et al., 2015), $BiVO_4$(Li et al., 2014), Bi_2WO_6(Li et al., 2018)), silver-based compounds (Ag_2O(Liang et al., 2019), Ag_3PO_4(Liu et al., 2016), Ag_3VO_4(Zhu et al., 2015)), multi-element rare Earth oxides (Zn_2GeO_4(Sun et al., 2014), $SrTiO_3$(Xu et al., 2011)), etc. The principle was executed in design of the heterojunction, that is, the recombination of g-C_3N_4 and the band-matched semiconductor promoted the transfer of charge carriers and suppressed the recombination of charges.

Based on different photogenerated carrier transfer mechanisms, the heterojunctions were formed when g-C_3N_4 coupled with other materials (Reza et al., 2015; Patnaik et al., 2016; Fu et al., 2018). In the heterojunction structures, Type-I constructure refers to that the position of CB of semiconductor-1 is higher than that of semiconductor-2, while the VB position of semiconductor-1 is lower than that of semiconductor-2, as shown in Figure 5A. Under the excitation of visible light, electrons and holes of the Type-I heterojunction photocatalyst are more inclined to migrate to the semiconductor-2 with a smaller band gap and undergo a redox reaction, and the separation efficiency of carriers is not significantly improved, resulting in the low rate of photocatalytic redox reaction. In the Type-II structure, the positions of both CB and VB of semiconductor-2 are lower than those of semiconductor-1, and therefore the photogenerated electrons and holes transferr into different sides of the heterostructure, as shown in Figure 5B. The carrier transport mode of the Type-II heterojunction greatly improve the photocatalytic activity of the composite photocatalyst. In 2021, Roy's team reported the TiO_2/ultrathin g-C_3N_4 (U-g-CN) heterostructure photocatalyst using a unique *in situ* thermal exfoliation process, and the presence of U-g-CN produced a redshift (~0.13eV) in the absorption edge of heterostructures compared to that of bare TiO_2, which extended the light absorption capability. Combined with the morphological characteristics of g-C_3N_4, Chen et al. prepared a novel 3D hierarchical hollow tubular g-C_3N_4/$ZnIn_2S_4$ nanosheets as the type-II heterojunction photocatalyst (Chen et al., 2022). The optimum photocatalyst offered the H_2 evolution rate up to 20,738 μmol h^{-1} g^{-1}. In the case of the Type-III heterojunction (Figure 5C), there are no any energy band intersection of semiconductor-1 and semiconductor-2, resulting in the inability of transport of photogenerated carriers between the semiconductors to greatly improve the photocatalytic efficiency.

Thus, a suitable semiconductor heterojunction is able to both enhance the ability to capture sunlight and significantly accelerate the separation and migration of photogenerated electron-hole pairs as description in Type II structure, but it is still insufficient in terms of photocatalytic oxidation ability. The Z-scheme heterojunction (Xu et al., 2022) was explored to overcome this disadvantage to a certain extent, which was mainly divided into binary and ternary structures, as shown in the Figure 6 (Maeda, 2013). The CB and VB potentials of

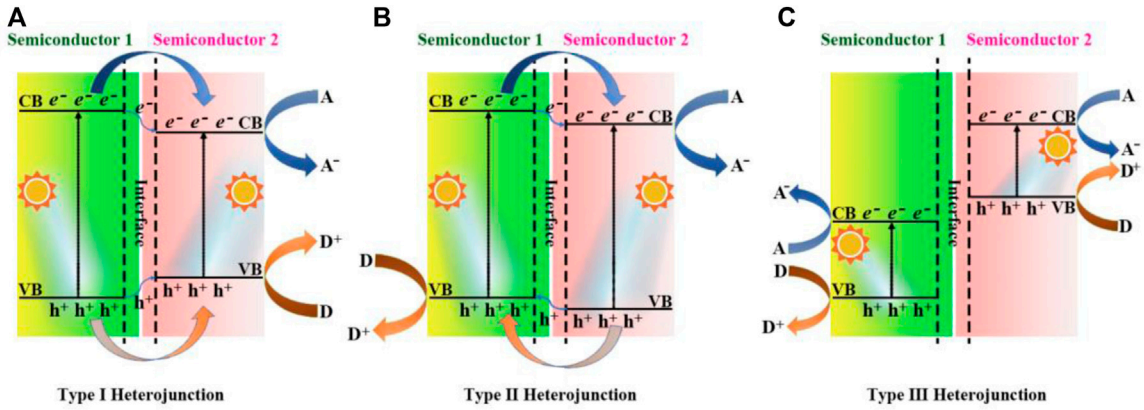

FIGURE 5
Schematic representation band structure of different heterojunctions: **(A)** Type I heterojunction; **(B)** Type II heterojunction; **(C)** Type III heterojunction. A and D represent electron acceptor and electron donor, respectively.

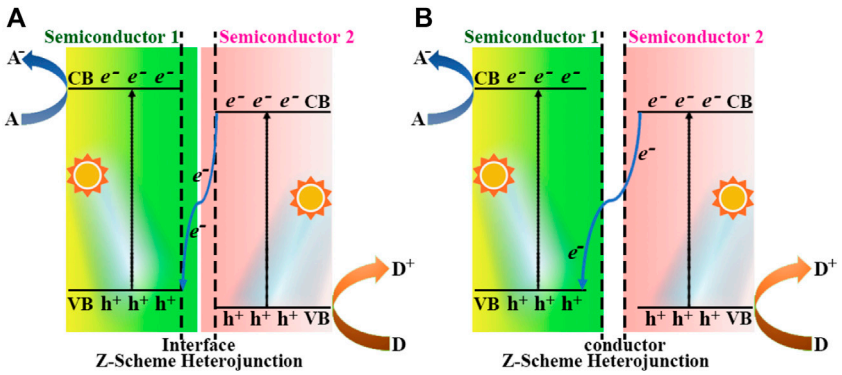

FIGURE 6
Schematic energy band diagram of two different types of Z-scheme heterojunction: **(A)** binary Z-scheme heterojunction, **(B)** ternary Z-scheme heterojunction. A and D denote electron acceptor and electron donor, respectively.

semiconductor-2 were more positive than those of semiconductor-1 in binary Z-scheme (Figure 6A), thereby enhancing the reduction and oxidation capacity of e^- and h^+. Zhao et al. prepared the CeO_2/g-C_3N_4 heterojunction photocatalysts, through a one-step *in situ* pyrolysis formation of 3D hollow CeO_2 mesoporous nanospheres and 2D g-C_3N_4 nanosheets. The hydrogen evolution from water splitting experiment of the CeO_2/g-C_3N_4-6 gave a maximum yield of 1,240.9 μmol g^{-1} h^{-1}, which was about 5.2 times higher than that of CeO_2 (Zhao et al., 2021). Figure 6B pictured out a conductor was employed as a charge bridge between the VB of semiconductor-1 and the CB of semiconductor-2 in the ternary Z-scheme heterojunction, which was played by metal particles, such as Cu, Au, Ag, etc. Hieu et al. synthesized the TiO_2/Ti_3C_2/g-C_3N_4 (TTC) photocatalyst from g-C_3N_4 and Ti_3C_2 MXene *via* a calcination technique, and a high H_2 production of 2,592 μmol g^{-1} was achieved (Hieu et al., 2021).

2.7 Homojunction structure

The g-C_3N_4 homojunctions are also recognized as the efficient photocatalysts. However, the type II structures and *Z*-schemes in the pioneering reports require deep optimization of the electron transport path in g-C_3N_4 homojunctions, since the redox potentials were depressed to inhibit the improvement of photocatalytic performance. The barrier could be overcome by the inspiration of *S*-scheme heterojunction proposed by Yu's group (Xu et al., 2020), Guo et al. fabricated the *S*-scheme homojunctions with high-crystalline/amorphous g-C_3N_4

(HCCN/ACN) with solvothermal method, which was applied in photocatalytic H_2 production with the evolution rates of 5.534 mmol h^{-1} g^{-1} in water and 3.147 mmol h^{-1} g^{-1} in seawater (Sun et al., 2022).

3 Conclusion

The excessive use and combustion of fossil fuels will inevitably bring some environmental problems. The value of hydrogen energy has been fully recognized, but its preparation technology still needs to be further explored. Photocatalytic technology is expected to realize sustainable energy production under the premise of making full use of solar energy, and has great potential in terms of energy and environment. The main factor limiting the photocatalytic activity of pristine g-C_3N_4 is its bulk structure, resulting in its small specific surface area and few active sites, which prolongs the transfer path of photogenerated electrons, thus accelerates the photogenerated charge carriers compound odds. The ability of photocatalytic hydrogen production performance of g-C_3N_4 could be improved by adjusting pH of the environment to induce the change of the surface charge of g-C_3N_4, controlling the morphology of g-C_3N_4 to increase active sites and shorten the transport path of carriers, and compositing co-catalysts or narrow-band semiconductors or dyes to enhance light absorption and reduce the recombination of photogenerated electrons and holes. So far, the strategies for exploration of stable hybridization structures to boost the photocatalytic efficiency could be the main concern in this filed, and more cases should be discovered to realize the dependence of the morphologies, structures, and species of dopants on the activities. This review is aimed at summarization of the recent progress of preparation and performance of g-C_3N_4-block photocatalysts to induce new ideas for the structural design with further improved efficiency by interdisciplinary researches across chemistry, physics, and material science.

Author contributions

R-HG, HC, and Y-QZ contributed to conception and design of the study. ML, QG, and NJ organized the database. R-HG wrote the first draft of the manuscript. All authors contributed to manuscript revision, read, and approved the submitted version.

Funding

This work was supported by Natural Science Foundation of Guizhou Province [No. ZK(2022)049], and National Natural Science Foundation of China (No. 22161011).

Conflict of interest

The authors declare that the research was conducted in the absence of any commercial or financial relationships that could be construed as a potential conflict of interest.

Publisher's note

All claims expressed in this article are solely those of the authors and do not necessarily represent those of their affiliated organizations, or those of the publisher, the editors and the reviewers. Any product that may be evaluated in this article, or claim that may be made by its manufacturer, is not guaranteed or endorsed by the publisher.

Supplementary material

The Supplementary Material for this article can be found online at: https://www.frontiersin.org/articles/10.3389/fchem.2022.1048504/full#supplementary-material

References

Bai, X. J., Wang, L., Zong, R. L., and Zhu, Y. (2013). Photocatalytic activity enhanced via g-C_3N_4 nanoplates to nanorods. *J. Phys. Chem. C* 117 (19), 9952–9961. doi:10.1021/jp402062d

Bard, A. J., and Fox, M. A. (1995). Artificial photosynthesis: Solar splitting of water to hydrogen and oxygen. *Acc. Chem. Res.* 28 (3), 141–145. doi:10.1021/ar00051a007

Bashir, H., Yi, X. Y., Yuan, J. L., Yin, K., and Luo, S. (2019). Highly ordered TiO_2 nanotube arrays embedded with g-C_3N_4 nanorods for enhanced photocatalytic activity. *J. Photochem. Photobiol. A Chem.* 382, 111930. doi:10.1016/j.jphotochem.2019.111930

Bi, L., Xu, D., Zhang, L., Lin, Y., Wang, D., and Xie, T. (2015). Metal Ni-loaded g-C_3N_4 for enhanced photocatalytic H_2 evolution activity: The change in surface band bending. *Phys. Chem. Chem. Phys.* 17 (44), 29899–29905. doi:10.1039/c5cp05158d

Caux, M., Menard, H., AlSalik, Y. M., Irvine, J. T. S., and Idriss, H. (2019). Photocatalytic hydrogen production over Au/g-C_3N_4: Effect of Gold Particle dispersion and morphology. *Phys. Chem. Chem. Phys.* 21 (29), 15974–15987. doi:10.1039/c9cp02241d

Chai, B., Liao, X., Song, F., and Zhou, H. (2014). Fullerene modified C_3N_4 composites with enhanced photocatalytic activity under visible light irradiation. *Dalton Trans.* 43 (3), 982–989. doi:10.1039/c3dt52454j

Chen, D., Wang, K., Hong, W., Zong, R., Yao, W., and Zhu, Y. (2015). Visible light photoactivity enhancement via CuTCPP hybridized g-C_3N_4 nanocomposite. *Appl. Catal. B Environ.* 166, 366–373. doi:10.1016/j.apcatb.2014.11.050

Chen, D., Wang, Z., Yue, D., Yang, G., Ren, T., and Ding, H. (2016). Synthesis and visible photodegradation enhancement of CdS/mpg-C_3N_4 photocatalyst. *J. Nanosci. Nanotechnol.* 16 (1), 471–479. doi:10.1166/jnn.2016.10661

Chen, H. B., and Liu, W. X. (2016). Cellulose-based photocatalytic paper with Ag_2O nanoparticles loaded on graphite fibers. *J. Bioresour. Bioprod.* 1 (4), 192–198. doi:10.21967/jbb.v1i4.63

Chen, P. W., Li, K., Yu, Y. X., and Zhang, W. De. (2017). Cobalt-doped graphitic carbon nitride photocatalysts with high activity for hydrogen evolution. *Appl. Surf. Sci.* 392, 608–615. doi:10.1016/j.apsusc.2016.09.086

Chen, X., Shi, R., Chen, Q., Zhang, Z., Jiang, W., Zhu, Y., et al. (2019). Three-dimensional porous g-C3N4 for highly efficient photocatalytic overall water splitting. *Nano Energy* 59, 644–650. doi:10.1016/j.nanoen.2019.03.010

Chen, X., Wei, J., Hou, R., Liang, Y., Xie, Z., Zhu, Y., et al. (2016). Growth of g-C_3N_4 on mesoporous TiO_2 spheres with high photocatalytic activity under visible light irradiation. *Appl. Catal. B Environ.* 188, 342–350. doi:10.1016/j.apcatb.2016.02.012

Chen, Z. H., Guo, F., Sun, H., Shi, Y. X., and Shi, W. L. (2022). Well-designed three-dimensional hierarchical hollow tubular g-C_3N_4/$ZnIn_2S_4$ nanosheets heterostructure for achieving efficient visible-light photocatalytic hydrogen evolution. *J. Colloid Interface Sci.* 607, 1391–1401. doi:10.1016/j.jcis.2021.09.095

Cui, L., Song, J., McGuire, A. F., Kang, S., Fang, X., Wang, J., et al. (2018). Constructing highly uniform onion-ring-like graphitic carbon nitride for efficient visible-light-driven photocatalytic hydrogen evolution. *ACS Nano* 12, 5551–5558. doi:10.1021/acsnano.8b01271

Dai, X., Jin, X. Y., Gao, R. H., Ge, Q., Chen, K., Jiang, N., et al. (2022). Controllable synthesis of Co nanoparticles with the assistance of cucurbit[6]uril and its efficient photoelectrochemical catalysis in water splitting on a g-C_3N_4 photoanode. *New J. Chem.* 46, 6738–6746. doi:10.1039/d2nj00036a

Deeksha, B., Sadanand, V., Hariram, N., and Rajulu, A. V. (2021). Preparation and properties of cellulose nanocomposite fabrics with *in situ* generated silver nanoparticles by bioreduction method. *J. Bioresour. Bioprod.* 6 (1), 75–81. doi:10.1016/j.jobab.2021.01.003

Di, J., Xiong, J., Li, H., and Liu, Z. (2018). Ultrathin 2D photocatalysts: Electronic-structure tailoring, hybridization, and applications. *Adv. Mat.* 30 (1), 1704548. doi:10.1002/adma.201704548

Fang, X. X., Ma, L. B., Liang, K., Zhao, S. J., Jiang, Y. F., Ling, C., et al. (2019). The Doping of phosphorus atoms into graphitic carbon nitride for highly enhanced photocatalytic hydrogen evolution. *J. Mat. Chem. A Mat.* 7 (18), 11506–11512. doi:10.1039/c9ta01646e

Fu, J., Yu, J., Jiang, C., and Cheng, B. (2018). g-C_3N_4-based heterostructured photocatalysts. *Adv. Energy Mat.* 8 (3), 1701503–1701531. doi:10.1002/aenm.201701503

Fujishima, A., and Honda, K. (1972). Electrochemical photolysis of water at a semiconductor electrode. *Nature* 238 (5358), 37–38. doi:10.1038/238037a0

Ge, L., and Han, C. (2012). Synthesis of MWNTs/g-C_3N_4 composite photocatalysts with efficient visible light photocatalytic hydrogen evolution activity. *Appl. Catal. B Environ.* 117, 268–274. doi:10.1016/j.apcatb.2012.01.021

Guo, F., Chen, Z., Huang, X., Cao, L., Cheng, X., Shi, W., et al. (2021). Cu_3P nanoparticles decorated hollow tubular carbon nitride as a superior photocatalyst for photodegradation of tetracycline under visible light. *Sep. Purif. Technol.* 275 (15), 119223. doi:10.1016/j.seppur.2021.119223

Guo, S., Deng, Z., Li, M., Jiang, B., Tian, C., Pan, Q., et al. (2016). Phosphorus-doped carbon nitride tubes with a layered micro-nanostructure for enhanced visible-light photocatalytic hydrogen evolution. *Angew. Chem. Int. Ed.* 55 (5), 1830–1834. doi:10.1002/anie.201508505

Han, Q., Wang, B., Zhao, Y., Hu, C., and Qu, L. (2015). A graphitic-C_3N_4 "seaweed" architecture for enhanced hydrogen evolution. *Angew. Chem. Int. Ed.* 54 (39), 11433–11437. doi:10.1002/anie.201504985

Hieu, V. Q., Lam, T. C., Khan, A., Thi Vo, T., Nguyen, T. Q., Doan, V. D., et al. (2021). TiO_2/Ti_3C_2/g-C_3N_4 ternary heterojunction for photocatalytic hydrogen evolution. *Chemosphere* 285, 131429. doi:10.1016/j.chemosphere.2021.131429

Indra, A., Menezes, P. W., Kailasam, K., Hollmann, D., Schroder, M., Thomas, A., et al. (2016). Nickel as a Co-catalyst for photocatalytic hydrogen evolution on graphitic-carbon nitride (sg-CN): What is the nature of the active species? *Chem. Commun.* 52 (1), 104–107. doi:10.1039/c5cc07936e

Kim, D., Sakimoto, K. K., Hong, D., and Yang, P. D. (2015). Artificial photosynthesis for sustainable fuel and chemical production. *Angew. Chem. Int. Ed.* 54 (11), 3259–3266. doi:10.1002/anie.201409116

Kong, L., Dong, Y., Jiang, P., Wang, G., Zhang, H., and Zhao, N. (2016). Light-assisted rapid preparation of a Ni/g-C_3N_4 magnetic composite for robust photocatalytic H_2 evolution from water. *J. Mat. Chem. A* 4 (25), 9998–10007. doi:10.1039/c6ta03178a

Kudo, A., and Miseki, Y. (2009). Heterogeneous photocatalyst materials for water splitting. *Chem. Soc. Rev.* 38 (1), 253–278. doi:10.1039/b800489g

Li, C., Wang, S., Wang, T., Wei, Y., Zhang, P., and Gong, J. (2014). Monoclinic porous $BiVO_4$ networks decorated by discrete g-C_3N_4 nano-islands with tunable coverage for highly efficient photocatalysis. *Small* 10 (14), 2783–2790. doi:10.1002/smll.201400506

Li, H. J., Qian, D. J., and Chen, M. (2015). Templateles infrared heating process for fabricating carbon nitride nanorods with efficient photocatalytic H_2 evolution. *ACS Appl. Mat. Interfaces* 7 (45), 25162–25170. doi:10.1021/acsami.5b06627

Li, H., Li, N., Wang, M., Zhao, B., and Long, F. (2018). Synthesis of novel and stable g-C_3N_4-Bi_2WO_6 hybrid nanocomposites and their enhanced photocatalytic activity under visible light irradiation. *R. Soc. open Sci.* 5 (3), 171419. doi:10.1098/rsos.171419

Li, Q., Zhang, N., Yang, Y., Wang, G., and Ng, D. H. L. (2014). High efficiency photocatalysis for pollutant degradation with MoS_2/C_3N_4 heterostructures. *Langmuir* 30 (29), 8965–8972. doi:10.1021/la502033t

Li, X., Yu, J., and Jaroniec, M. (2016). Hierarchical photocatalysts. *Chem. Soc. Rev.* 45 (9), 2603–2636. doi:10.1039/c5cs00838g

Liang, S., Zhang, D., Pu, X., Yao, X., Han, R., Yin, J., et al. (2019). A novel Ag_2O/g-C_3N_4 p-n heterojunction photocatalysts with enhanced visible and near-infrared light activity. *Sep. Purif. Technol.* 210, 786–797. doi:10.1016/j.seppur.2018.09.008

Lin, Z., and Wang, X. (2014). Ionic liquid promoted synthesis of conjugated carbon nitride photocatalysts from urea. *ChemSusChem* 7 (6), 1547–1550. doi:10.1002/cssc.201400016

Liu, E., Lin, X., Hong, Y., Yang, L., Luo, B., Shi, W., et al. (2021). Rational copolymerization strategy engineered C self-doped g-C_3N_4 for efficient and robust solar photocatalytic H_2 evolution. *Renew. Energy* 178, 757–765. doi:10.1016/j.renene.2021.06.066

Liu, L., Qi, Y., Lu, J., Lin, S., An, W., Liang, Y., et al. (2016). A stable Ag_3PO_4@g-C_3N_4 hybrid core@shell composite with enhanced visible light photocatalytic degradation. *Appl. Catal. B Environ.* 183, 133–141. doi:10.1016/j.apcatb.2015.10.035

Liu, Q., Li, N., Qiao, Z., Li, W., Wang, L., Zhu, S., et al. (2019). The multiple promotion effects of ammonium phosphate-modified Ag_3PO_4 on photocatalytic performance. *Front. Chem.* 7, 866. doi:10.3389/fchem.2019.00866

Liu, S., Zada, A., Yu, X., Liu, F., and Jin, G. (2022). $NiFe_2O_4$/g-C_3N_4 heterostructure with an enhanced ability for photocatalytic degradation of tetracycline hydrochloride and antibacterial performance. *Chemosphere* 307, 135717. doi:10.1016/j.chemosphere.2022.135717

Liu, Y., Kang, S., Cui, L., and Ma, Z. (2020). Boosting near-infrared-driven photocatalytic H_2 evolution using protoporphyrin-sensitized g-C_3N_4. *J. Photochem. Photobiol. A Chem.* 396, 112517–112526. doi:10.1016/j.jphotochem.2020.112517

Maeda, K., Teramura, K., Lu, D., Takata, T., Saito, N., Inoue, Y., et al. (2006). Photocatalyst releasing hydrogen from water. *Nature* 440 (7082), 295. doi:10.1038/440295a

Maeda, K. (2013). Z-scheme water splitting using two different semiconductor photocatalysts. *ACS Catal.* 3 (7), 1486–1503. doi:10.1021/cs4002089

Min, S., and Lu, G. (2012). Enhanced electron transfer from the excited eosin Y to mpg-C_3N_4 for highly efficient hydrogen evolution under 550 nm irradiation. *J. Phys. Chem. C* 116 (37), 19644–19652. doi:10.1021/jp304022f

Mo, Z., Xu, H., Chen, Z. G., She, X., Song, Y., Wu, J., et al. (2018). Self-assembled synthesis of defect-engineered graphitic carbon nitride nanotubes for efficient conversion of solar energy. *Appl. Catal. B Environ.* 225, 154–161. doi:10.1016/j.apcatb.2017.11.041

Nagajyothi, P. C., Pandurangan, M., Vattikuti, S. V. P., Tettey, C. O., Sreekanth, T. V. M., and Shim, J. (2017). Enhanced photocatalytic activity of Ag/g-C_3N_4 composite. *Sep. Purif. Technol.* 188, 228–237. doi:10.1016/j.seppur.2017.07.026

Nagaraja, C. M., Kaur, M., and Dhingra, S. (2020). Enhanced visible-light-assisted photocatalytic hydrogen generation by MoS_2/g-C_3N_4 nanocomposites. *Int. J. Hydrogen Energy* 45 (15), 8497–8506. doi:10.1016/j.ijhydene.2020.01.042

Naseri, A., Samadi, M., Pourjavadi, A., Moshfegh, A. Z., and Ramakrishma, S. (2017). Graphitic carbon nitride (g-C_3N_4)-based photocatalysts for solar hydrogen generation: Recent advances and future development directions. *J. Mat. Chem. A Mat.* 5 (45), 23406–23433. doi:10.1039/c7ta05131j

Niu, P., Zhang, L., Liu, G., and Cheng, H. M. (2012). Graphene-like carbon nitride nanosheets for improved photocatalytic activities. *Adv. Funct. Mat.* 22 (22), 4763–4770. doi:10.1002/adfm.201200922

Ong, W. J., Tan, L. L., Ng, Y. H., Yong, S. T., and Chai, S. P. (2016). Graphitic carbon nitride (g-C3N4)-based photocatalysts for artificial photosynthesis and environmental remediation: Are we a step closer to achieving sustainability? *Chem. Rev.* 116 (12), 7159–7329. doi:10.1021/acs.chemrev.6b00075

Ou, M., Wan, S., Zhong, Q., Zhang, S., and Wang, Y. (2017). Single Pt atoms deposition on g-C_3N_4 nanosheets for photocatalytic H_2 evolution or NO oxidation under visible light. *Int. J. Hydrogen Energy* 42 (44), 27043–27054. doi:10.1016/j.ijhydene.2017.09.047

Patnaik, S., Martha, S., and Parida, K. M. (2016). An overview of the structural, textural and morphological modulations of g-C_3N_4 towards photocatalytic hydrogen production. *RSC Adv.* 6 (52), 46929–46951. doi:10.1039/c5ra26702a

Qi, K., Cui, N., Zhang, M., Ma, Y., Wang, G., Zhao, Z., et al. (2021). Ionic liquid-assisted synthesis of porous boron-doped graphitic carbon nitride for photocatalytic hydrogen production. *Chemosphere* 272, 129953. doi:10.1016/j.chemosphere.2021.129953

Qi, K., Li, Y., Xie, Y., Liu, S., Zheng, K., Chen, Z., et al. (2019). Ag loading enhanced photocatalytic activity of g-C_3N_4 porous nanosheets for decomposition of organic pollutants. *Front. Chem.* 7, 91. doi:10.3389/fchem.2019.00091

Qi, K., Liu, S., and Zada, A. (2020). Graphitic carbon nitride, a polymer photocatalyst. *J. Taiwan Inst. Chem. Eng.* 109, 111–123. doi:10.1016/j.jtice.2020.02.012

Qi, K., Lv, W., Khan, I., and Liu, S. (2020). Photocatalytic H_2 generation via CoP quantum-dot-modified g-C_3N_4 synthesized by electroless plating. *Chin. J. Catal.* 41 (1), 114–121. doi:10.1016/s1872-2067(19)63459-5

Qi, K., Zhang, C., Zhang, M., Gholami, P., and Khataee, A. (2022). Sonochemical synthesis of photocatalysts and their applications. *J. Mat. Sci. Technol.* 123, 243–256. doi:10.1016/j.jmst.2022.02.019

Qi, Y., Xu, J., Zhang, M., Lin, H., and Wang, L. (2019). *In situ* metal-organic framework-derived C-doped Ni_3S_4/Ni_2P hybrid co-catalysts for photocatalytic H_2 production over g-C_3N_4 via dye sensitization. *Int. J. Hydrogen Energy* 44 (31), 16336–16347. doi:10.1016/j.ijhydene.2019.04.276

Ran, J., Ma, T. Y., Gao, G., Du, X. W., and Qiao, S. Z. (2015). Porous P-doped graphitic carbon nitride nanosheets for synergistically enhanced visible-light photocatalytic H_2 production. *Energy Environ. Sci.* 8 (12), 3708–3717. doi:10.1039/c5ee02650d

Reza, G. M., Dinh, C. T., Beland, F., and Do, T. O. (2015). Nanocomposite heterojunctions as sunlight-driven photocatalysts for hydrogen production from water splitting. *Nanoscale* 7 (18), 8187–8208. doi:10.1039/c4nr07224c

Samanta, S., Martha, S., and Parida, K. (2014). Facile synthesis of Au/g-C_3N_4 nanocomposites: An inorganic/organic hybrid plasmonic photocatalyst with enhanced hydrogen gas evolution under visible-light irradiation. *ChemCatChem* 6 (5), 1453–1462. doi:10.1002/cctc.201300949

Schwinghanmmer, K., Tuffy, B., Mesch, M. B., Wirnhier, E., Martineau, C., Taulelle, F., et al. (2013). Triazine-based carbon nitrides for visible-light-driven hydrogen evolution. *Angew. Chem. Int. Ed.* 52 (9), 2435–2439. doi:10.1002/anie.201206817

Shen, X. C., Tang, Y. J., Zhou, D. D., Zhang, J. H., Guo, D. L., and Friederichs, G. (2016). Improving the electroconductivity and mechanical properties of cellulosic paper with multi-walled carbon nanotube/polyaniline nanocomposites. *J. Bioresour. Bioprod.* 1 (1), 48–54. doi:10.21967/jbb.v1i1.40

Shi, W. L., Sun, W., Liu, Y., Li, X. Y., Lin, X., Guo, F., et al. (2022). Onion -ring-like g-C_3N_4 modified with Bi_3TaO_7 quantum dots: A novel 0D/3D S-scheme heterojunction for enhanced photocatalytic hydrogen production under visible light irradiation. *Renew. Energy* 182, 958–968. doi:10.1016/j.renene.2021.11.030

Shi, Y., Jiang, S., Zhou, K., Wang, B., Wang, B., Gui, Z., et al. (2014). Facile Preparation of ZnS/g-C_3N_4 nanohybrids for enhanced optical properties. *RSC Adv.* 4 (6), 2609–2613. doi:10.1039/c3ra44256j

Shi, Y. X., Li, L. L., Sun, H. R., Xu, Z., Cai, Y., Shi, W. L., et al. (2022). Engineering ultrathin oxygen-doped g-C_3N_4 nanosheet for boosted photoredox catalytic activity based on a facile thermal gas-shocking exfoliation effect. *Sep. Purif. Technol.* 292, 121038. doi:10.1016/j.seppur.2022.121038

Sun, H., R., Wang, L. J., Guo, F., Shi, Y. X., Li, L. L., Xu, Z., et al. (2022a). Fe-doped g-C_3N_4 derived from biowaste material with Fe-N bonds for enhanced synergistic effect between photocatalysis and Fenton degradation activity in a broad pH range. *J. Alloys Compd.* 900, 163410. doi:10.1016/j.jallcom.2021.163410

Sun, H. R., Shi, Y. X., Shi, W. L., and Guo, F. (2022b). High-crystalline/amorphous g-C_3N_4 S-scheme homojunction for boosted photocatalytic H_2 production in water/simulated seawater: Interfacial charge transfer and mechanism insight. *Appl. Surf. Sci.* 593, 153281. doi:10.1016/j.apsusc.2022.153281

Sun, J. X., Yuan, Y. P., Qiu, L. G., Jiang, X., Xie, A. J., Shen, Y. H., et al. (2012). Fabrication of composite photocatalyst g-C_3N_4-ZnO and enhancement of photocatalytic activity under visible light. *Dalton Trans.* 41 (22), 6756–6763. doi:10.1039/c2dt12474b

Sun, L., Qi, Y., Jia, C. J., Jin, Z., and Fan, W. (2014). Enhanced visible-light photocatalytic activity of g-C_3N_4/Zn_2GeO_4 heterojunctions with effective interfaces based on band match. *Nanoscale* 6 (5), 2649–2659. doi:10.1039/c3nr06104c

Sun, X. H., Shi, Y. X., Lu, J. L., Shi, W. L., and Guo, F. (2022). Template-free self-assembly of three-dimensional porous graphitic carbon nitride nanovesicles with size-dependent photocatalytic activity for hydrogen evolution. *Appl. Surf. Sci.* 606, 154841. doi:10.1016/j.apsusc.2022.154841

Theerthagiri, J., Senthil, R. A., Priya, A., Madhavan, J., Michael, R. J. V., and Ashokkumar, M. (2014). Photocatalytic and photoelectrochemical studies of visible-light active alpha-Fe_2O_3-g-C_3N_4 nanocomposites. *RSC Adv.* 4 (72), 38222–38229. doi:10.1039/c4ra04266b

Thomas, A., Fischer, A., Goettmann, F., Antonietti, M., Muller, J. O., Schlogl, R., et al. (2008). Graphitic carbon nitride materials: Variation of structure and morphology and their use as metal-free catalysts. *J. Mat. Chem.* 18 (41), 4893–4908. doi:10.1039/b800274f

Wang, B., Wang, Y., Lei, Y., Wu, N., Gou, Y., Han, C., et al. (2016). Mesoporous silicon carbide nanofibers with *in situ* embedded carbon for Co-catalyst free photocatalytic hydrogen production. *Nano Res.* 9 (3), 886–898. doi:10.1007/s12274-015-0971-z

Wang, L. X., Zhao, F., Han, Q., Hu, C., Lv, L., Chen, N., et al. (2015). Spontaneous formation of Cu_2O-g-C_3N_4 core-shell nanowires for photocurrent and humidity responses. *Nanoscale* 7 (21), 9694–9702. doi:10.1039/c5nr01521a

Wang, P., Guan, Z., Li, Q., and Yang, J. (2018). Efficient visible-light-driven photocatalytic hydrogen production from water by using Eosin Y-sensitized novel g-C_3N_4/Pt/GO composites. *J. Mat. Sci.* 53 (1), 774–786. doi:10.1007/s10853-017-1540-5

Wang, Q., Hisatomi, T., Jia, Q., Tokudome, H., Zhao, M., Wang, C., et al. (2016). Scalable water splitting on particulate photocatalyst sheets with a solar-to-hydrogen energy conversion efficiency exceeding 1%. *Nat. Mat.* 15 (6), 611–615. doi:10.1038/nmat4589

Wang, W., Yu, J. C., Shen, Z., Chan, D. K. L., and Gu, T. (2014). g-C_3N_4 quantum dots: direct synthesis, upconversion properties and photocatalytic application. *Chem. Commun.* 50 (70), 10148–10150. doi:10.1039/c4cc02543a

Wang, X., Maeda, K., Thomas, A., Takanabe, K., Xin, G., Carlsson, J. M., et al. (2009). A metal-free polymeric photocatalyst for hydrogen production from water under visible light. *Nat. Mat.* 8 (1), 76–80. doi:10.1038/nmat2317

Wang, Y., Hong, J., Zhang, W., and Xu, R. (2013). Carbon nitride nanosheets for photocatalytic hydrogen evolution: Remarkably enhanced activity by dye sensitization. *Catal. Sci. Technol.* 3 (7), 1703–1711. doi:10.1039/c3cy20836b

Wang, Z., Xu, X., Si, Z., Liu, L., He, Y., Ran, R., et al. (2018). *In situ* synthesized MoS_2/Ag dots/Ag_3PO_4 Z-scheme photocatalysts with ultrahigh activity for oxygen evolution under visible light irradiation. *Appl. Surf. Sci.* 450, 441–450. doi:10.1016/j.apsusc.2018.04.149

Wu, P., Wang, J., Zhao, J., Guo, L., and Osterloh, F. E. (2014). High alkalinity boosts visible light driven H_2 evolution activity of g-C_3N_4 in aqueous methanol. *Chem. Commun.* 50 (98), 15521–15524. doi:10.1039/c4cc08063g

Wu, X., Zhu, C., Wang, L., Guo, S., Zhang, Y., Li, H., et al. (2017). Control strategy on two-/four-electron pathway of water splitting by multidoped carbon based catalysts. *ACS Catal.* 7 (3), 1637–1645. doi:10.1021/acscatal.6b03244

Xiang, Q., Yu, J., and Jaroniec, M. (2011). Preparation and enhanced visible-light photocatalytic H_2 production activity of graphene/C_3N_4 composites. *J. Phys. Chem. C* 115 (15), 7355–7363. doi:10.1021/jp200953k

Xiao, N., Li, Y., Li, X., Gao, Y., Ge, L., Lu, G., et al. (2019). *In-situ* synthesis of PdAg/g-C_3N_4 composite photocatalyst for highly efficient photocatalytic H_2 generation under visible light irradiation. *Int. J. Hydrogen Energy* 44 (36), 19929–19941. doi:10.1016/j.ijhydene.2019.05.236

Xu, J., Qi, Y., Wang, W., and Wang, L. (2019). Montmorillonite-hybridized g-C_3N_4 composite modified by NiCoP cocatalyst for efficient visible-light-driven photocatalytic hydrogen evolution by dye-sensitization. *Int. J. Hydrogen Energy* 44 (8), 4114–4122. doi:10.1016/j.ijhydene.2018.12.167

Xu, Q., Zhang, L., Cheng, B., Fan, J., and Yu, J. (2020). S-scheme heterojunction photocatalyst. *Chem* 6 (7), 1543–1559. doi:10.1016/j.chempr.2020.06.010

Xu, X., Liu, G., Randorn, C., and Irvine, J. T. S. (2011). g-C_3N_4 coated $SrTiO_3$ as an efficient photocatalyst for H_2 production in aqueous solution under visible light irradiation. *Int. J. Hydrogen Energy* 36 (21), 13501–13507. doi:10.1016/j.ijhydene.2011.08.052

Xu, Z., Shi, Y. X., Li, L. L., Sun, H., R., Amin, M. D. S., Guo, F., et al. (2022). Fabrication of 2D/2D Z-scheme highly crystalline carbon nitride/δ-Bi_2O_3 heterojunction photocatalyst with enhanced photocatalytic degradation of tetracycline. *J. Alloys Compd.* 895, 162667. doi:10.1016/j.jallcom.2021.162667

Yu, L., Zhang, X., Zhuang, C., Lin, L., Li, R., and Peng, T. (2014). Syntheses of asymmetric zinc phthalocyanines as sensitizer of Pt-loaded graphitic carbon nitride for efficient visible/near-IR-light-driven H_2 production. *Phys. Chem. Chem. Phys.* 16 (9), 4106–4114. doi:10.1039/c3cp54316a

Yue, B., Li, Q., Iwai, H., Kako, T., and Ye, J. (2011). Hydrogen production using zinc-doped carbon nitride catalyst irradiated with visible light. *Sci. Technol. Adv. Mat.* 12 (3), 034401034401–034401/7. doi:10.1088/1468-6996/12/3/034401

Zada, A., Khan, M., Qureshi, M. N., Liu, S. Y., and Wang, R. D. (2019). Accelerating photocatalytic hydrogen production and pollutant degradation by functionalizing g-C_3N_4 with SnO_2. *Front. Chem.* 7, 941. doi:10.3389/fchem.2019.00941

Zeng, Y., Liu, X., Liu, C., Wang, L., Xia, Y., Zhang, S., et al. (2018). Scalable one-step production of porous oxygen-doped g-C_3N_4 nanorods with effective electron separation for excellent visible-light photocatalytic activity. *Appl. Catal. B Environ.* 224, 1–9. doi:10.1016/j.apcatb.2017.10.042

Zhang, G., Zhang, M., Ye, X., Qiu, X., Lin, S., and Wang, X. (2014). Iodine modified carbon nitride semiconductors as visible light photocatalysts for hydrogen evolution. *Adv. Mat.* 26 (5), 805–809. doi:10.1002/adma.201303611

Zhang, J. Y., Wang, Y. H., Jin, J., Lin, Z., Huang, F., Yu, J. G., et al. (2013). Efficient visible-light photocatalytic hydrogen evolution and enhanced photostability of core/shell CdS/g-C_3N_4 nanowires. *ACS Appl. Mat. Interfaces* 5 (20), 10317–10324. doi:10.1021/am403327g

Zhang, P., Song, T., Wang, T., and Zeng, H. (2017). Effectively extending visible light absorption with a broad spectrum sensitizer for improving the H_2 evolution of *in-situ* Gu/g-C_3N_4 nanocomponents. *Int. J. Hydrogen Energy* 42 (21), 14511–14521. doi:10.1016/j.ijhydene.2017.04.234

Zhang, P., Wang, T., and Zeng, H. (2017). Design of Cu-Cu_2O/g-C_3N_4 nanocomponent photocatalysts for hydrogen evolution under visible light irradiation using water-soluble Erythrosin B dye sensitization. *Appl. Surf. Sci.* 391, 404–414. doi:10.1016/j.apsusc.2016.05.162

Zhang, S., Khan, I., Qin, X., Qi, K., Liu, Y., and Bai, S. (2020). Construction of 1D Ag-AgBr/AlOOH plasmonic photocatalyst for degradation of tetracycline hydrochloride. *Front. Chem.* 8, 117. doi:10.3389/fchem.2020.00117

Zhang, X., Peng, B., Zhang, S., and Peng, T. (2015). Robust wide visible-light-responsive photoactivity for H_2 production over a polymer/polymer heterojunction photocatalyst: The significance of sacrificial reagent. *ACS Sustain. Chem. Eng.* 3 (7), 1501–1509. doi:10.1021/acssuschemeng.5b00211

Zhang, X., Peng, T., Yu, L., Li, R., Li, Q., and Li, Z. (2015). Visible/near-infrared-light-induced H_2 production over g-C_3N_4 Co-sensitized by organic dye and zinc phthalocyanine derivative. *ACS Catal.* 5 (2), 504–510. doi:10.1021/cs5016468

Zhang, X. W., Zhu, Y. F., Chen, X. Q., Shen, W. H., and Lutes, R. (2018). How does binuclear zinc amidohydrolase FwdA work in the initial step of methanogenesis: From formate to formyl-methanofuran. *J. Inorg. Biochem.* 3 (2), 71–79. doi:10.1016/j.jinorgbio.2018.05.004

Zhang, X., Yu, L., Zhuang, C., Peng, T., Li, R., and Li, X. (2014). Highly asymmetric phthalocyanine as a sensitizer of graphitic carbon nitride for extremely efficient photocatalytic H_2 production under near-infrared light. *ACS Catal.* 4 (1), 162–170. doi:10.1021/cs400863c

Zhang, Y., Liu, J., Wu, G., and Chen, W. (2012). Porous graphitic carbon nitride synthesized via direct polymerization of urea for efficient sunlight-driven photocatalytic hydrogen production. *Nanoscale* 4 (17), 5300–5303. doi:10.1039/c2nr30948c

Zhao, S., Xu, J., Mao, M., Li, L., and Li, X. (2021). Protonated g-C_3N_4 cooperated with Co-MOF doped with Sm to construct 2D/2D heterojunction for integrated dye-sensitized photocatalytic H_2 evolution. *J. Colloid Interface Sci.* 583, 435–447. doi:10.1016/j.jcis.2020.09.063

Zhao, S., Zhang, Y. W., Zhou, Y. M., Wang, Y., Qiu, K., Zhang, C., et al. (2018). Facile one-step synthesis of hollow mesoporous g-C_3N_4 spheres with ultrathin nanosheets for photoredox water splitting. *Carbon* 126, 247–256. doi:10.1016/j.carbon.2017.10.033

Zhao, W., She, T., Zhang, J., Wang, G., Zhang, S., Wei, W., et al. (2021). A novel z-scheme CeO_2/g-C_3N_4 heterojunction photocatalyst for degradation of bisphenol A and hydrogen evolution and insight of the photocatalysis mechanism. *J. Mater. Sci. Technol.* 85, 18–29. doi:10.1016/j.jmst.2020.12.064

Zhao, Y., Zada, A., Yang, Y., Pan, J., Wang, Y., Yan, Z., et al. (2021). Photocatalytic removal of antibiotics on g-C_3N_4 using amorphous CuO as cocatalysts. *Front. Chem.* 9, 797738. doi:10.3389/fchem.2021.797738

Zhong, X., Wang, G., Papandrea, B., Li, M., Xu, Y., Chen, Y., et al. (2015). Reduced graphene oxide/silicon nanowire heterostructures with enhanced photoactivity and superior photoelectrochemical stability. *Nano Res.* 8 (9), 2850–2858. doi:10.1007/s12274-015-0790-2

Zhu, T., Song, Y., Ji, H., Xu, Y., Song, Y., Xia, J., et al. (2015). Synthesis of g-C_3N_4/Ag_3VO_4 composites with enhanced photocatalytic activity under visible light irradiation. *Chem. Eng. J.* 271, 96–105. doi:10.1016/j.cej.2015.02.018

Zhu, Y., Wang, T., Xu, T., Li, Y., and Wang, C. (2019). Size effect of Pt co-catalyst on photocatalytic efficiency of g-C_3N_4 for hydrogen evolution. *Appl. Surf. Sci.* 464, 36–42. doi:10.1016/j.apsusc.2018.09.061

Zhuang, J., Zhang, J., Pang, J., Wang, A., Wang, X., and Zhu, W. (2019). Fabrication of pyrimidine/g-C_3N_4 nanocomposites for efficient photocatalytic activity under visible-light illumination. *Dyes Pigments* 163, 634–640. doi:10.1016/j.dyepig.2018.12.046

Zou, X., Dong, Y., Li, X., Zhao, Q., Cui, Y., and Lu, G. (2015). Inorganic-organic photocatalyst $BiPO_4$/g-C_3N_4 for efficient removal of gaseous toluene under visible light irradiation. *Catal. Commun.* 69, 109–113. doi:10.1016/j.catcom.2015.04.035